

# Channelling flows in the Hunter Valley

 Christopher Webb<sup>A</sup> and Jiwon Park<sup>B,\*</sup> 

For full list of author affiliations and declarations see end of paper

## \*Correspondence to:

 Jiwon Park  
NSW and ACT Decision Support Service,  
Bureau of Meteorology, Sydney, NSW,  
Australia  
Email: [jiwon.park@bom.gov.au](mailto:jiwon.park@bom.gov.au)

## Handling Editor:

Brad Murphy

## ABSTRACT

The Hunter Valley is well known for the strong westerly winds in winter and elevated fire danger arising from hot and dry north-westerly winds in summer. These hazards are closely related to the valley channelling in the region, and the connection between the two has been an interest to weather forecasters, emergency service personnel, and the aviation industry. In this paper, the climatology of valley winds is constructed to identify the dominant types of channelling in the Hunter Valley and their preferred directions using the 10-year data of Automatic Weather Station observations, upper air sounding and ERA5 reanalysis data between July 2010 and June 2020. Particular attention is given to the conceptual model of pressure-driven channelling of westerlies in winter and its mechanics, as the climatology shows that it is the main cause of wind-warning conditions in the Hunter.

**Keywords:** channelling flows, climatology, Hunter funnelling, Hunter Valley, Newcastle, pressure-driven channelling, severe weather, valley channelling, Williamtown.

## 1 Introduction

The interaction of an approaching airstream with topography within a valley leads to the channelling of winds along the orientation of the valley. Valley channelling has been observed over much of the globe, including the Upper Rhine Valley in Germany (Gross and Wippermann 1987), the Tennessee Valley in the USA (Whiteman and Doran 1993) and a series of deep valleys in the mountainous region around Basel, Switzerland (Weber and Kaufmann 1998) to name a few. Research in valley channelling has been undertaken in application to the dispersion of air pollution (Whiteman and Doran 1993; Weber and Kaufmann 1998) and its relationship to significant weather events, including strong winds (Zhong *et al.* 2008) and freezing rain and ice storms (Carrera *et al.* 2009). As a part of an effort to solve these problems, those papers mention climatological studies undertaken to determine the prevailing type(s) of channelling for the valley concerned, or numerical simulations to understand its mechanism.

The Hunter Valley is a broad river valley in central eastern New South Wales, Australia. The valley is an important industrial and agricultural area with a population of more than half a million around the city of Newcastle. The valley is prone to strong westerly winds in winter and hot and dry north-westerly winds with a risk of elevated fire danger in summer. The region is also prone to easterly winds associated with a high pressure system over the Tasman Sea (Tasman High), often posing a significant aviation hazard with widespread fog and low clouds. These meteorological features and hazards are closely connected to the channelling in the Hunter Valley, and in view of the importance of the region to the Australian economy, the authors believe that a study on this topic can benefit the general public and industries in the region while serving as a useful reference to the emergency services in New South Wales. In the first part, we aim to construct the climatology of valley channelling in the Hunter Valley and identify the prevailing channelling types using wind roses and joint-probability distribution diagrams of geostrophic and valley winds. In the second part, particular attention will be given to the amplification of strong westerly winds through the Hunter Valley, known as ‘Hunter funnelling’, because of its importance to wind warnings to the public and the aviation industry. Funnelling is a term used by weather forecasters in Australia to denote the

Received: 17 July 2022

Accepted: 19 July 2023

Published: 1 August 2023

## Cite this:

 Webb C and Park J (2023)  
*Journal of Southern Hemisphere Earth  
Systems Science*  
73(2), 194–211. doi:[10.1071/ES22021](https://doi.org/10.1071/ES22021)

 © 2023 The Author(s) (or their  
employer(s)). Published by  
CSIRO Publishing on behalf of the Bureau  
of Meteorology.

 This is an open access article distributed  
under the Creative Commons Attribution-  
NonCommercial-NoDerivatives 4.0  
International License ([CC BY-NC-ND](https://creativecommons.org/licenses/by-nc-nd/4.0/))

OPEN ACCESS

topographic enhancement of winds (prevailing westerly or northerly in Australia) through a valley or a mountain gap. The second part will aim to investigate the type of valley channelling that causes Hunter funnelling and its mechanics using a conceptual model and a supporting case study. Although hazards associated with valley channelling from other directions are equally important and interesting as they pose their unique hazards, they will not be discussed here.

## 2 Data and methods

### 2.1 Topography of the Hunter Valley and the surface-level observation from the Bureau of Meteorology's Automatic Weather Station network

Fig. 1 depicts the topography of the Hunter Valley and surrounding regions, with the key observation sites denoted by blue squares. The Hunter Valley is part of a 250-km-long corridor from the opening of the Great Dividing Range in the Central West Slopes and Plains (CWSP) to the Hunter Coast, and the width ranges between 30 and 70 km, with a gentle downward gradient from west to east. The valley is oriented

ESE–WNW ( $\sim 115\text{--}295^\circ$ ), perpendicular to the Great Dividing Range, which runs parallel to the New South Wales coastline along NNE–SSW, and it is bounded by the Liverpool Ranges and Barrington Tops to the north, and the higher ground of the Central Tablelands to the south. The elevations of the mountain ranges that form the valley walls are  $\sim 500\text{--}1000$  m above mean sea level, with the highest location Barrington Tops being  $\sim 1400\text{--}1500$  m high and several smaller valleys running from these mountain ranges. The Upper Hunter is the higher side in the west with an elevation ranging between 200 and 400 m above mean sea level. The area includes the townships of Scone (aviation code YSCO, elevation 221 m), Merriwa (MERW, 375 m) and Muswellbrook, and Dunedoo in its western end. The corridor gradient continues sloping upward to the west of the Upper Hunter, reaching the highest elevation of  $\sim 400$  to 500 m in higher parts of CWSP between Cassilis and Dunedoo, forming the opening of the Great Dividing Range before sloping down towards the western slopes and inland plains. To the east, the region gently slopes downwards, with an average angle of inclination of 0.002 radians, and meets the Hunter coastline. The eastern side of the corridor is called the Lower Hunter, and it encompasses the Newcastle Metropolitan Area, including the Newcastle CBD at the river

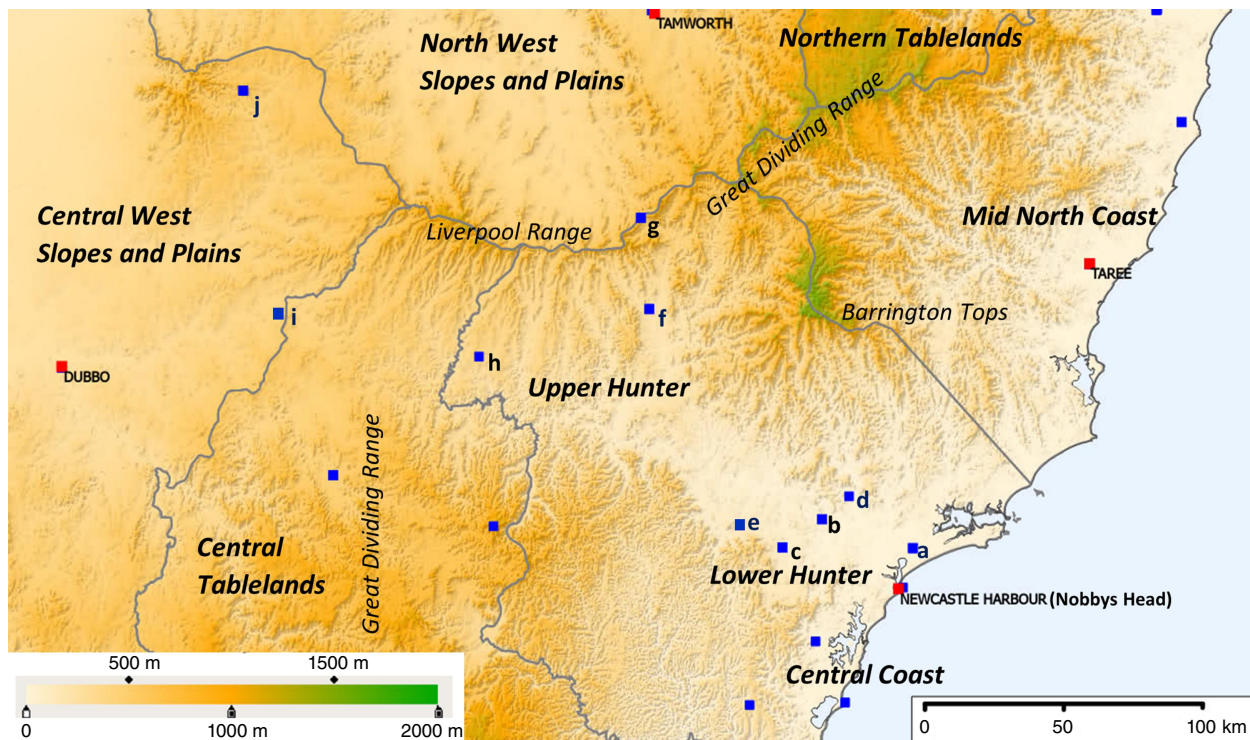


**Fig. 1.** Topography of the Hunter Valley and surrounding regions with major cities or regional centres (red squares) and key observation sites or townships (blue squares). Major towns include (with aviation code and observation site elevation): Newcastle Harbour and Nobbys Head (NBB, 33.0 m) and Dubbo (YSDU, 284 m). Key observation sites are (a) Williamtown RAAF base (YWLM, 7.5 m), (b) Maitland (YMND, 27.5 m), (c) Cessnock (YCNK, 66.5 m), (d) Tocal (TOC, 30.0 m), (e) Singleton (SNGL, 125 m), (f) Scone (YSCO, 221 m), (g) Murrurundi Gap (MUI, 729 m), (h) Merriwa (MERW 375 m), (i) Dunedoo (YDNO, 388 m), (j) Coonabarabran (YCBB, 645 m). The grey lines indicate the Bureau's forecast district boundaries.

mouth of the Hunter River, Newcastle Harbour near Nobbys Head (NBB, 33.0 m), Williamtown Royal Australian Air Force (RAAF) base and airport (YWLM, 7.5 m) ~10 km to the north of the city, the township of Maitland (YMND, 27.5 m) ~30 km to the north-west of the city, and the winery region around Cessnock. Historically, the Hunter Valley designates the river valley formed along the Hunter River – the main river in the region that flows from Barrington Tops to Newcastle Harbour via Muswellbrook. In this work, however, the whole corridor between Dunedoo and Newcastle will be denoted as the *main valley* as the flow in the Hunter region is largely constricted by this corridor within the Great Dividing Range, and the valley channelling will be discussed chiefly in the context of the main valley.

The Bureau of Meteorology (henceforth, ‘the Bureau’) operates an observation office at Williamtown RAAF base and several Automatic Weather Stations (AWSs) in the Hunter region. Among them, the observations from Williamtown, Nobbys Head, Maitland and Merriwa will be particularly important as these stations are distributed nearly along the axis of the main valley. Observations from Scone, Dubbo (YSDU, 284 m) and Coonabarabran (YCBB, 645 m) are also of particular interest, although these sites are away from the axis. Observations from Cessnock (YCNK, 66.5 m) and Tocal (TOC, 30.0 m) will only be considered when tallying high-end events since these sites are relatively shielded from westerlies because of blocking hills and their locations away from the valley axis. The AWS anemometers with 10-m masts record the gust wind speed by taking the samples every 3 s. The highest gust speed for a day is recorded as the daily maximum wind gust. The weather stations also report Mean Sea Level Pressure (MSLP), 10-min mean winds and 10-min peak gusts, and other weather elements at every 3-h interval as surface synoptic observations (SYNOPS). The Bureau’s dataset of 10-year SYNOPS and the records of daily maximum wind gusts between July 2010 and June 2020 will be used to construct the climatology of valley winds. Also of particular interest is evaluating  $\Delta p$  – the pressure difference across the two ends of the valley (hPa). As for the reference value at the valley’s eastern end, SYNOP MSLP at Williamtown RAAF will be used. There is no nearby AWS site at the western end (~20 km to the north of Dunedoo), but it is about the centroid of a triangle formed by Merriwa, Dubbo and Coonabarabran. Hence the MSLP at the western end is estimated to be the mean MSLP of these three AWS sites. With this,  $\Delta p$  is:

$$\Delta p = \frac{1}{3}(p_{(\text{Merriwa})} + p_{(\text{Dubbo})} + p_{(\text{Coonabarabran})}) - p_{(\text{Williamtown})}$$

This will be used extensively in Section 4 in connection to the wind speeds in the Lower Hunter.

The AWSs also report 10-min mean winds and the maximum of the samples in the 10-min period at every 30-min

interval as meteorological aerodrome report (METAR) wind or gust. Non-routine aviation selected special weather reports (SPECIS) are also made when special conditions are met regarding visibility, cloud base or variation of wind speeds and directions. METAR and SPECI (or 1-min data when wind directions or speeds change rapidly within certain time intervals) will be used to construct the time series of wind speeds and directions for case studies. Over the coastal waters, satellite-derived winds from an advanced scatterometer (ASCAT) will be used as a proxy of METAR winds when ASCAT passes coincide with the time of interest, with a caveat that ASCAT winds are only an approximation to the actual wind speeds.

## 2.2 Types of valley channelling and the upper-level wind data used

Whiteman and Doran (1993) classified the types of valley channelling into the following four categories.

### 2.2.1 Thermal forcing

In the absence of a significant synoptic forcing, a locally developed thermal wind system controls valley winds. The temperature difference within the valley produces an along-valley pressure gradient, and this causes the valley winds to follow the diurnal cycle, up-valley during the day and down-valley during the night. Winds driven by thermal forcing tend to be stronger in deep, narrow valleys than in wide valleys with low valley walls (Whiteman and Doran 1993; Weber and Kaufmann 1998). In the Hunter Valley, thermally forced valley winds seldom exceed 10 knots (~18.5 km h<sup>-1</sup>) as the valley belongs to the latter category. Although it is an interesting local wind effect, it will not be considered in detail, since the focus of this paper is on the valley channelling in response to synoptic forcing.

### 2.2.2 Downward momentum transport

The valley winds follow the directions of geostrophic winds due to the downward momentum transport of upper-level winds by turbulent mixing. This mechanism is most likely to occur under statically unstable or neutral conditions (Zhong *et al.* 2008). When this happens, a slight turning of wind directions by ~25° toward lower pressure is expected at the ground level due to the frictional drag. It is commonly observed in wide, flat-bottomed valleys with low sidewalls, as this mechanism involves no modification of wind directions by topography (Whiteman and Doran 1993).

### 2.2.3 Forced channelling

In this mechanism, the valley winds originating from the upper-level winds by downward momentum transport are forced to align with the valley axis due to the anisotropic friction from valley walls (Weber and Kaufmann 1998). Forced channelling is commonly observed in deep and

narrow valleys under unstable or neutral conditions. Valley wind directions shift by  $180^\circ$  when the geostrophic wind directions cross the line perpendicular to the valley axis.

### 2.2.4 Pressure-driven channelling

The valley winds are driven by the pressure gradient along the valley axis. This pressure gradient is distinguished from the thermally induced pressure gradient within the valley discussed in a), in the sense that it is at a larger scale than the valley itself. This tends to be observed in wide and shallow valleys under moderately stable conditions (Wippermann 1984; Gross and Wippermann 1987; Whiteman and Doran 1993). Valley wind directions shift by  $180^\circ$  when the geostrophic wind directions cross the valley axis.

Fig. 2 shows an idealised relationship between valley wind directions and geostrophic wind directions in the

four types of valley channelling, adapted from Whiteman and Doran (1993) in the context of the Hunter Valley, which is located in the Southern Hemisphere. To identify the prevailing type(s) of valley channelling in the Hunter Valley, joint-probability distributions of valley wind directions (10-m level winds) against 850-hPa wind directions are constructed in Section 3, and then they are compared with Fig. 2 to identify the primary channelling type in the Hunter in each season. The 850-hPa winds were chosen as a proxy for geostrophic winds because this level lies higher than the mean altitude of the nearby mountain ranges ( $\sim 1000$  m) while being close to the gradient level of the higher parts of the main valley. The 850-hPa winds in the Lower Hunter were obtained from the upper air sounding at Williamtown RAAF base ( $32.79^\circ\text{S}$ ,  $151.84^\circ\text{E}$ ) as the station conducts daily upper air sounding at 23Z, that is 09:00 hours Australian Eastern Standard Time (AEST, +10 Coordinated Universal Time, UTC). In the case of missing Williamtown observations, 00Z 850-hPa winds at

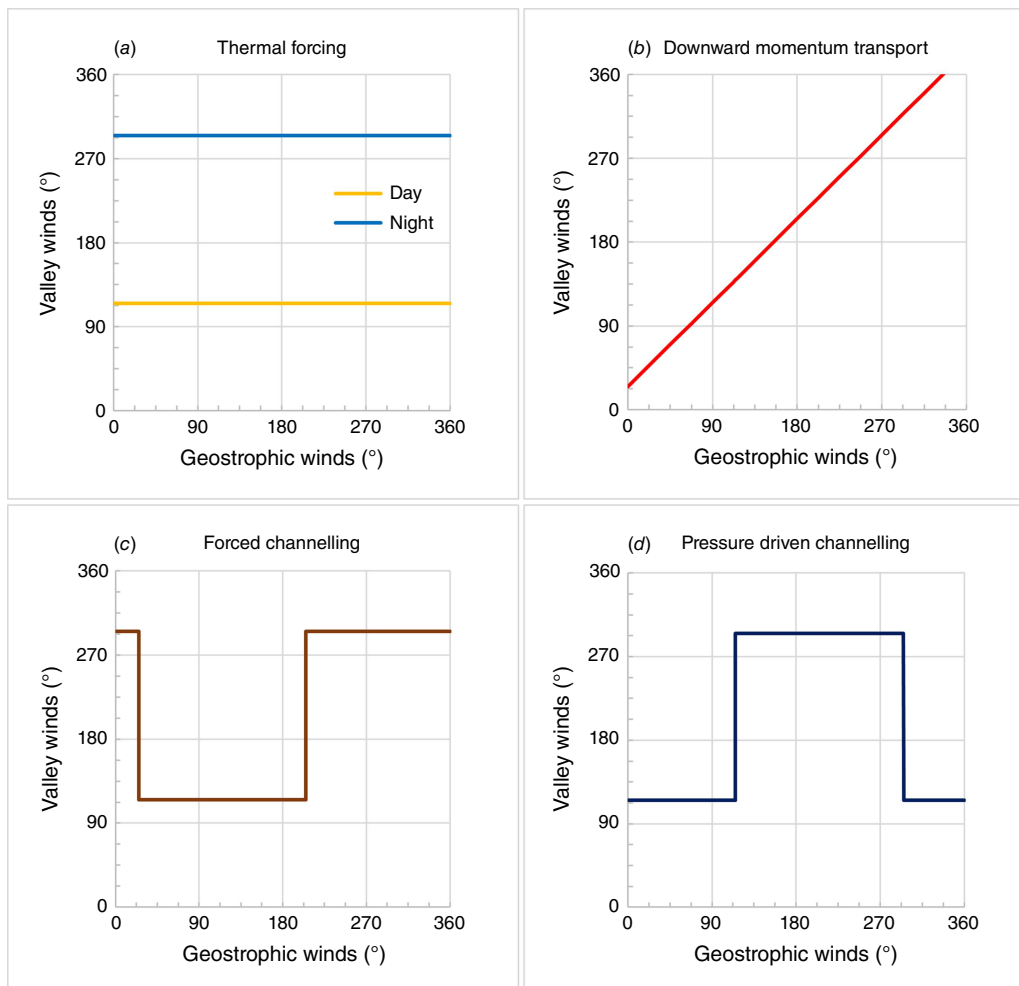


**Fig. 2.** Relationship between valley wind directions v. geostrophic wind directions for four types of valley channelling, (a) thermal forcing, (b) downward momentum transport, (c) forced channelling, (d) pressure-driven channelling, in the context of the Hunter Valley where the valley is oriented ESE–WNW ( $115\text{--}295^\circ$ ).

32.90°S, 151.75°E (near Newcastle) from the ECMWF ERA5 reanalysis dataset (Muñoz Sabater 2019; Hersbach *et al.* 2020) – or simply *reanalysis data* from now on – were used instead. As there is no nearby station conducting upper air sounding in the Upper Hunter, 850-hPa reanalysis winds at 32.25°S, 150.25°E (near Merriwa) were used as the site lies at the centre of the Upper Hunter along the valley axis. The upper-level wind data were discarded for speeds less than 3 knots ( $\sim 5 \text{ km h}^{-1}$ ) as the wind directions can be variable with light winds.

### 3 Seasonal, spatial and directional variations of valley channelling in the Hunter Valley

In New South Wales, heat and moisture drive the weather patterns between October and March, with risks of elevated fire danger or severe thunderstorms. By contrast, the cold and dry westerly airstreams drive the weather patterns between April and September. For this reason, October to March marks the severe weather season for the forecasting offices and the emergency services in New South Wales (State Emergency Service, SES, and Rural Fire Service, RFS), whereas April to September is considered a non-severe weather season. For convenience, we define the *summer season* as October to March and the *winter season* as April to September. The seasonal variation of the dominant channelling type, or the preferred channelling type for each geostrophic wind direction, and subsequent valley winds in the Hunter Valley arise due to the difference in the air mass involved and its associated atmospheric stability or instability. Also, spatial variation in the dominant channelling type occurs between the Upper and Lower Hunter due to the difference in the local topography, with a relatively narrower valley width in the Upper Hunter than in the Lower Hunter. In this section, the seasonal, spatial and directional variation of the valley winds and associated channelling type(s) are investigated with the aid of the joint-probability distributions of the valley wind directions *v.* geostrophic wind directions.

Fig. 3 and 4 are the joint-probability distributions of 10-m level wind directions (valley wind) *v.* the 850-hPa wind directions (geostrophic wind) for the Upper and the Lower Hunter respectively, constructed by the method described in Section 2.2 using the 10-year data between July 2010 and June 2020. The prevailing wind directions were manually inserted as dashed grey lines as a guide. The dataset of 850-hPa winds was already described in Section 2, and they (or geostrophic winds) will be referred to as *airstreams*. Also, the interval of wind directions will be denoted in a clockwise direction. As the diurnal variation of thermally forced valley winds will not be considered separately, 06:00-, 09:00- and 12:00-hours SYNOP winds (that is, SYNOP within 3 h of Williamstown upper air sounding) are all used in the plots, with 06:00-hours winds representing

down-valley katabatic winds whereas 12:00-hours winds representing thermally forced up-valley winds as well as winds by downward momentum transport by daytime heating. It is also assumed that, in most cases, the directions of the geostrophic winds did not change significantly within 3 h before or after the upper air sounding, so the use of upper air winds at one single time step is justified.

Inspection of the joint-probability distributions in the Upper Hunter (Fig. 3) reveals that:

- (1) Fig. 3a, c shows pronounced characteristics of downward momentum transport by turbulent mixing with SW–NNW airstreams in summer, as the valley winds follow the directions of upper-level winds within this interval apart from slight veering from 850-hPa wind directions by  $\sim 25^\circ$ . This is consistent with known characteristics of wide, flat-bottomed valleys (Whiteman and Doran 1993).
- (2) Fig. 3b (Merriwa in winter) most resembles the ideal plot of pressure-driven channelling (Fig. 2d), except that the  $180^\circ$  swing of valley wind directions occurs slightly off the valley axis by  $\sim 20^\circ$ . This deviation of swinging directions from the valley axis is likely due to the asymmetry of valley walls or mountain gaps (Whiteman and Doran 1993). Scone in winter displays a similar pattern to Merriwa (Fig. 3d), except that it shows a mix of pressure-driven channelling and downward momentum transport with S–NNW airstreams.
- (3) Valley winds in the Upper Hunter display a strong signature of SE channelling with NNW–SE airstreams in both summer and winter. Because the  $180^\circ$  shift of valley wind directions occurs at NNW, which is not far from the valley's axis, the channelling with NNW–SE airstreams in the Upper Hunter is likely due to pressure-driven channelling. The same SE channelling associated with SE–SSW airstreams in summer (Fig. 3a, c) is attributed to forced channelling as it extends beyond the orientation of the valley axis. The channelling direction in Merriwa follows the orientation of the main valley (ESE), whereas Scone shows southerly bias due to the orientation of its own valley along the N–S direction.
- (4) Fig. 3a, c shows the local maxima of the probability of SE valley winds with W–NW airstreams in summer. It appears to indicate the existence of a counter-current in the Hunter Valley, a unique feature of pressure-driven channelling (Wippermann 1984; Gross and Wippermann 1987), although a minor contribution from thermally forced up-valley winds under weak W–NW synoptic flow cannot be ruled out. Fig. 3b, d also displays similar local maxima in winter, but the signal is much weaker.

The connection between each channelling type and preferred atmospheric stability was surveyed in Section 2.2.1–2.2.4, and the synoptic feature or air mass involved for each channelling direction can be inferred from this.

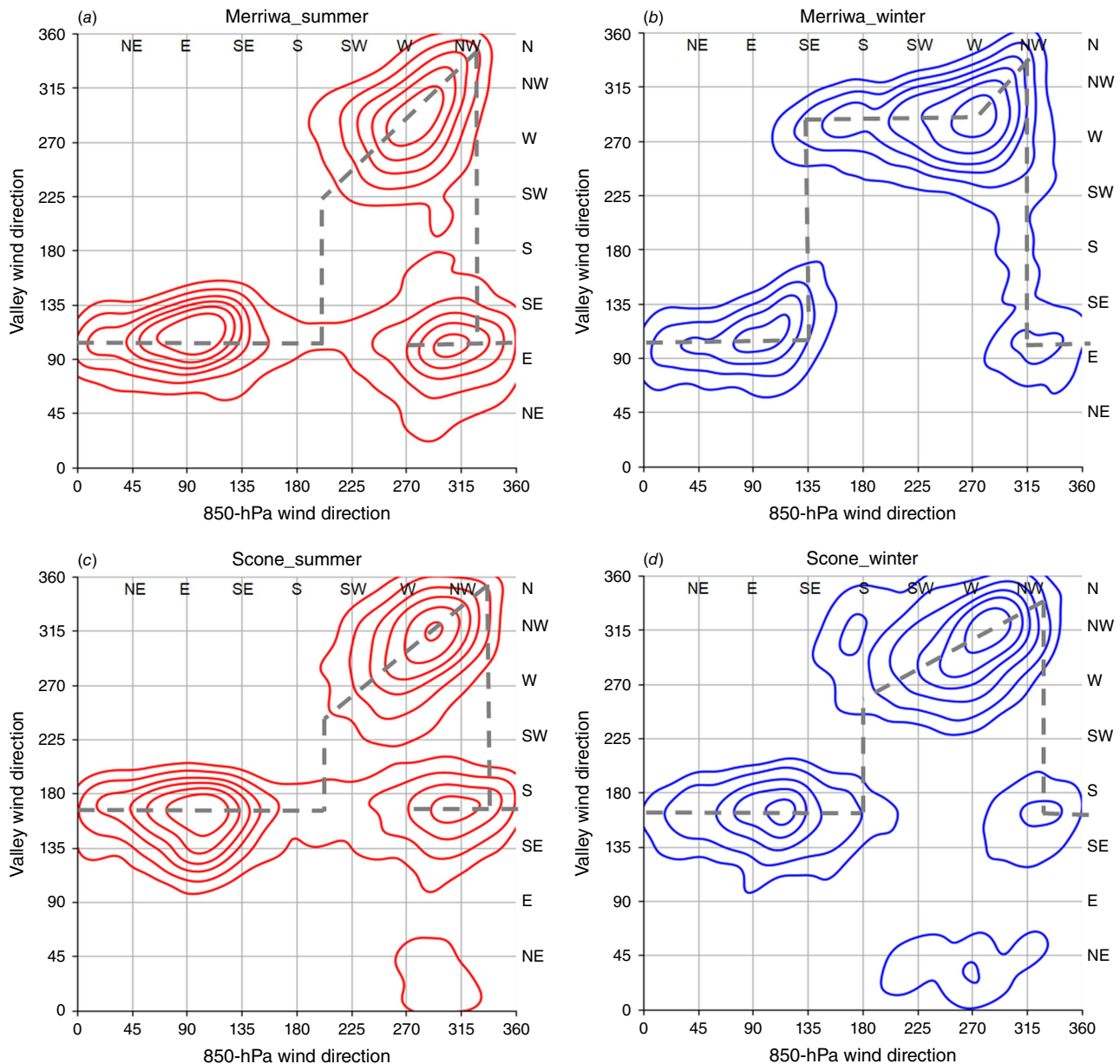


**Fig. 3.** Joint-probability distributions of valley wind directions and 850-hPa wind directions in the Upper Hunter based on the 10-year data between July 2010 and June 2020. (a) Merriwa in summer, (b) Merriwa in winter, (c) Scone in summer, (d) Scone in winter. Valley winds are 06:00-, 09:00- and 12:00-hours SYNOP 10-m winds. The 850-hPa winds are 00Z reanalysis winds at 32.25°S, 150.25°E. Contours are isolines of the marginal probability density at 15, 30, 45, 60, 75 and 90%.

Point (1) discussed the strong signature of downward momentum transport in summer. Fig. 3a, c show the peak within W–NW airstreams, and this arises from unstable or neutral atmospheric stability and turbulent mixing within a deep boundary layer in connection with a hot continental air mass from central Australia. This air mass is characterised by a strong thermal ridge that sometimes extends to New South Wales with airstreams from the NW quadrant. This implies that the Upper Hunter and nearby areas of CWSP along the main valley are subject to a high risk of

elevated fire danger during summer with hot and dry conditions, especially in El Niño years. Additionally, fire danger may escalate to extreme or catastrophic fire danger when a low to mid-level jet in the pre-front mixes down to the surface by downward momentum transport. The Sir Ivan Fire in February 2017 was the most notable example of such conditions in the region in recent years (Australian Institute for Disaster Resilience 2017). By contrast, the signatures of pressure-driven channelling associated with SE valley winds and moderate to stable atmospheric stability

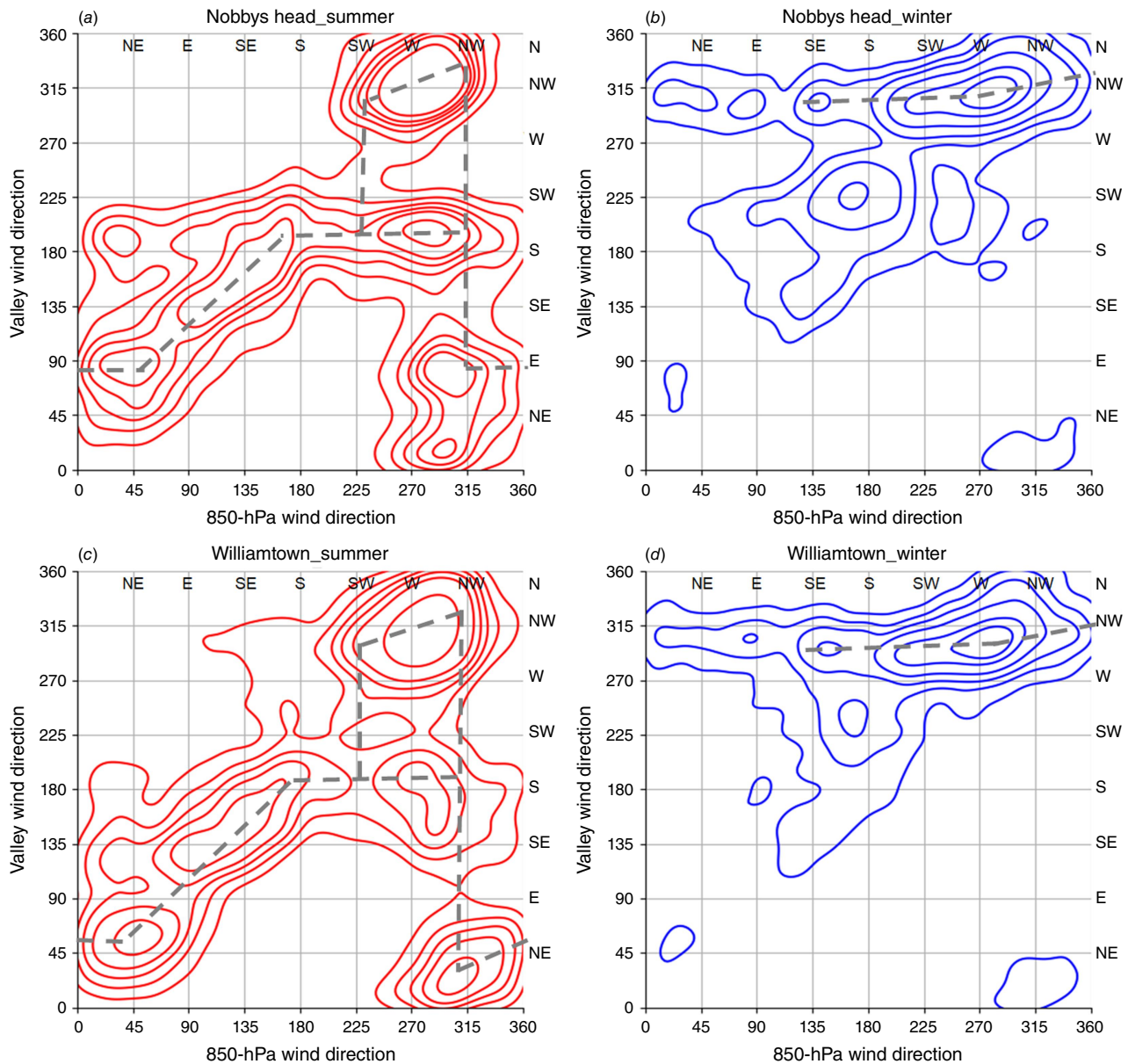


**Fig. 4.** Joint-probability distributions of valley wind directions and 850-hPa wind directions in the Lower Hunter during the same period. (a) Nobbys Head in summer, (b) Nobbys Head in winter, (c) Williamtown in summer, (d) Williamtown in winter. Valley winds are 06:00-, 09:00- and 12:00-hours SYNOP 10-m winds. The 850-hPa winds are 23Z Williamtown sounding (or 00Z reanalysis winds in the absence). Contours are isolines of the marginal probability densities at 15, 30, 45, 60, 75 and 90%.

implied in (3)–(4) can be attributed to Tasman High, which often forms to the east of the valley. The system is well known for bringing widespread fog or low clouds in eastern New South Wales (Matthews *et al.* 2002), and the Hunter Valley is no exception.

Likewise, the following observations can be made regarding the joint-probability distribution in the Lower Hunter (Fig. 4).

(5) The channelling directions in summer with NNW–S airstreams are less distinct in the Lower Hunter than the

Upper Hunter due to a wider spread of observations in Fig. 4a, c than in Fig. 3a, c. However, such a spread is expected due to the broader valley width in the Lower Hunter than in the Upper Hunter, with a wide opening of the Lower Hunter facing the Hunter coastline to the east. The maritime influence, such as sea breeze or coastal southerly change, together with valley channeling, complicates the prevailing wind directions in the area. In Fig. 4a, c, the E–NE winds at the surface level with NW–NE airstreams in summer are due to sea-breeze circulation. The surface wind directions associated with

NE–S airstreams in summer display characteristics of downward momentum transport. This is due to the turbulent mixing of maritime easterly winds or post-frontal SE–S airstreams. As pointed out in (3), the same airstreams show a strong signature of channelling (pressure-driven or forced) along the valley axis when they reach the Upper Hunter (Fig. 3a, c).

- (6) Fig. 4a, c displays two main surface wind directions with SW–NW airstreams: one along NW and the other along S directions. In summer, SW quadrant airstreams bring a post-frontal air mass to the Upper Hunter from inland and it reaches the coast as SE–S wind changes due to the Great Dividing Range. Such deflection is evident in Fig. 4a, c since they show that the post-frontal air mass can reach the Lower Hunter as both NW winds channelled through the valley or as a coastal southerly change. The true direction of valley channelling is NW winds in this regard. The veering of the valley winds from the orientation of the valley (WNW) to NW in the Lower Hunter is likely due to the frictional drag. When the W–NW valley winds in the Lower Hunter are compared with the valley winds in the Upper Hunter under the same conditions in summer (Fig. 3a, c), the Lower Hunter shows a stronger signature of valley channelling than the Upper Hunter.
- (7) The NW channelling stands out in winter (Fig. 4b, d). The dominance of down-valley drainage flow under weak synoptic forcing, lack of sea breeze development in winter, and frequent passage of cold fronts are thought to contribute to this. High densities of NW channelling are notable through SE–NNW airstreams in Fig. 4b, d, and this interval's channelling type(s) can be both pressure driven and forced according to Fig. 2c, d. Still, due to the lack of E–SE winds at the surface level in winter, the joint-probability distributions are inconclusive on the primary channelling type, especially in the overlapping interval of SSW–WNW airstreams.
- (8) The secondary maxima of SSW winds at the surface level with S airstream in winter (Fig. 4b, d) are due to the maritime synoptic systems such as East Coast Low (ECL), Tasman Low or a coastal southerly wind change after a cold front.

As (7) is inconclusive, winter season NW valley channelling in the Lower Hunter requires further consideration of other factors. The following arguments support pressure-driven channelling as the primary channelling type in the overlapping interval of SSW–WNW airstream in winter.

- (a) Fig. 3b, d shows that the westerly airstream in winter is mainly pressure driven in the upstream region (Upper Hunter). The valley width widens towards the Lower Hunter as the NW winds channel through the valley. Therefore anisotropic friction at the valley walls has less influence upon the valley winds – hence less room for

topographic constriction and forced channelling – in the Lower Hunter than in the Upper Hunter. Wide valleys with low valley walls favour pressure-driven channelling (Gross and Wippermann 1987; Whiteman and Doran 1993), whereas deep and narrow valleys favour forced channelling (Weber and Kaufmann 1998; Zhong *et al.* 2008). The Hunter Valley falls into the former category.

- (b) The geostrophic wind from the SW quadrant means a high-pressure system to the NW and a low-pressure system to the SE of the valley. Such a synoptic setup creates a pressure gradient between the eastern and western sides of the valley (i.e. between the Lower and Upper Hunter). The effect of the pressure gradient is manifest by the wind-max (the area of maximum wind speed at the surface level) around Newcastle and nearby coastal waters (which will be discussed in Section 4).

The pressure-driven channelling of NW valley winds in winter is of particular interest because of its connection to the wind-warning conditions in the Lower Hunter. It will be discussed further in the next section. Despite the reasoning in (a) and (b), some minority of NW channelling events could still be attributed to forced channelling, downward momentum transport or even a mix of the two when the atmosphere is less stable. This is more so with WNW–NNW airstreams, as this interval is outside the interval of pressure-driven channelling (Fig. 2d).

#### 4 Hazard associated with the winter season westerlies in the Hunter Valley

The valley channelling of westerly winds in the Hunter Valley is most conspicuous in winter, especially in the Lower Hunter (Fig. 4b, d). The valley channelling may bring wind-warning conditions in the Hunter Valley provided: (a) the airstream entering the valley is from the due west, or its direction does not deviate much from the west, and (b) a strong pressure gradient exists between the two ends of the valley. The first part of this section will begin with a case study illustrating this point, then it will be followed by a climatology of wind-warning conditions to verify (a). The third part will be devoted to the conceptual model to understand the overall mechanics of such wind events and demonstrate (b) by finding the relationship between the pressure gradient force and the maximum wind speeds expected in the valley. As we restrict our attention only to the channelling of westerly winds from now on, the western end of the valley will be denoted simply as the *entrance* and the eastern end as the *exit* of the valley.

##### 4.1 Case study I: 6 July 2016

The Bureau issues a severe weather warning for damaging winds if a synoptic system is forecast (or observed) to bring

*gale-force winds* (10-min mean winds exceeding 33 knots or  $\sim 60 \text{ km h}^{-1}$ ) or *damaging wind gusts* (gusts exceeding 48 knots or  $\sim 90 \text{ km h}^{-1}$ ). Similarly, an aerodrome warning is issued for Williamstown RAAF if the wind gusts are forecast to exceed 42 knots ( $\sim 77.8 \text{ km h}^{-1}$ ). The 6 July 2016 event met the criteria for both a severe weather warning (winds) and an aerodrome warning for Williamstown. A low-pressure system and its associated front moved across eastern New South Wales on 5 July 2016. The following day (6 July), the primary low centre slowly moved to the Tasman Sea and deepened, with a secondary centre forming off the South Coast. A post-frontal synoptic W–SW flow affected much of eastern New South Wales, producing a strong pressure gradient between the Upper and Lower

Hunter. The synoptic forcing remained almost steady due to the blocking high over the Bight cradling the low. Fig. 5a–d are the time series of the AWS surface-level winds across the Hunter Valley and  $\Delta p$  for the 24-h period between 00:00 hours on 6 July and 00:00 hours on 7 July. Winds were strong and gusty even from the early morning in the wake of a cold front that passed the day before. Except for Scone, wind directions remained nearly along the valley axis (between 280 and 300°) throughout the period, even though the wind direction at Dubbo gradually backed from W–WNW to SW–W through the afternoon (Fig. 5c). Wind directions in the Lower Hunter remained WNW–NW, veering  $\sim 10\text{--}15^\circ$  from the valley axis much of the period, likely due to frictional drag. Scone remained N–NW until the

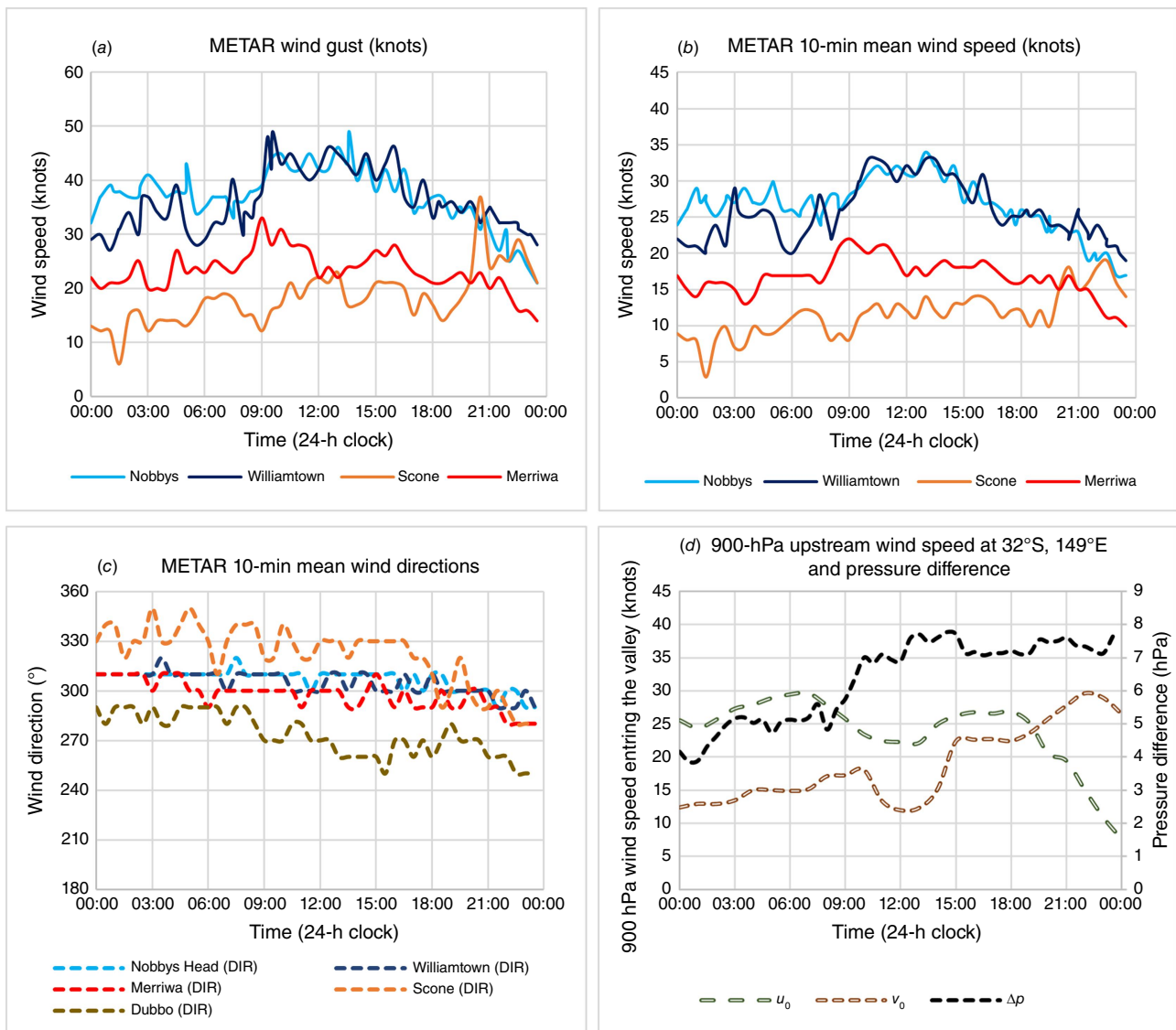


**Fig. 5.** Time series of METAR observations at Nobbys Head, Williamstown, Scone and Merriwa, and 900-hPa reanalysis winds at the entrance from 00:00 hours on 6 July to 00:00 hours on 7 July 2016: (a) time series of gust speeds, (b) time series of mean wind speeds, (c) time series of wind directions, (d) time series of  $u_0$ ,  $v_0$  at  $32.00^\circ\text{S}$ ,  $149.00^\circ\text{E}$  from reanalysis data and  $\Delta p$  from surface observations.

evening because of the mountain gap winds channelling through its own valley from Murrurundi, and its speed remained weaker than Merriwa until the evening. According to Fig. 5a, b, the wind speeds in the Lower Hunter stations (YWLM, NBB, YMND) were  $\sim 1.5$ – $2.5$  times stronger than those at Upper Hunter stations (MERW, YSCO) throughout the day. Shown in Fig. 6 are the METAR map and the isotachs of surface-level winds at 00Z (10:00 hours AEST), which reinforces this observation. The isotachs were manually analysed every 15 knots ( $\sim 27.8 \text{ km h}^{-1}$ ) from the METAR and ASCAT winds, and the narrow wind-max region around Newcastle and the nearby coastal waters can be seen. The temporal evolution of the event can also be seen in Fig. 5d, which shows the time series of the pressure differences  $\Delta p$  defined in Section 2.1, and  $u_0$ ,  $v_0$  – the along-valley component ( $u_0$ ) and the normal component ( $v_0$ ) of the 900-hPa reanalysis wind at the entrance ( $32.00^\circ\text{S}$ ,  $149.00^\circ\text{E}$ ). The wind speeds in the Lower Hunter (Fig. 5a, b) closely followed the variation of  $\Delta p$  until c. 16:00 hours, with a sharp increase of wind speeds at NBB and YWLM following the steep rise of  $\Delta p$  by  $\sim 2$  hPa between 08:00 and 10:00 hours. To evaluate the contribution of thermal forcing to  $\Delta p$ , the increase in the 900-hPa temperature contrast between the Upper and the Lower Hunter between 08:00 and 14:00 hours AEST was investigated, and it was found to be only  $\sim 1^\circ\text{C}$  according to reanalysis data, which translates to an  $\sim 0.4$ -hPa increase by

hydrostatic balance. By contrast, the central pressure of the low off the South Coast that drove the channelling flow in the Hunter Valley deepened from 1001 to 994 hPa between 10:00 and 16:00 hours. Hence the increase in  $\Delta p$  during the morning and early afternoon was mainly due to the increase in synoptic forcing with the deepening of the low. At c. 09:00 hours, the 10-min mean wind speeds at both YWLM and NBB reached near-gale strength (30 knots,  $\sim 55.6 \text{ km h}^{-1}$ ) and remained so until c. 16:00 hours, with the peak wind gust 49 knots ( $\sim 91 \text{ km h}^{-1}$ ) recorded at YWLM at 09:30 hours and the same peak gust at NBB at 13:30 hours. These observations are also consistent with the 23Z (09:00 hours AEST) Williamtown upper air sounding in Fig. 7, which shows a low-level jet reaching 50–55 knots ( $\sim 92.6$ – $101.8 \text{ km h}^{-1}$ ) between 950 and 850 hPa underneath the inversion at 850 hPa. It also shows that the depth of the well-mixed boundary layer was close to 1000 m at 09:00 hours AEST with a super-adiabatic shallow layer near surface level when the low-level jet started to mix down. As the screen temperatures in the Lower Hunter increased to mid-teens during the day (YWLM recorded  $14.9^\circ\text{C}$  at 12:00 hours), it can be inferred from the sounding that the depth of the well-mixed boundary layer grew to  $\sim 1500$  m by early afternoon while maintaining the speed of the jet underneath the inversion. Although the pressure difference between the Upper and Lower Hunter remained steady after 16:00 hours, the valley winds in the Lower

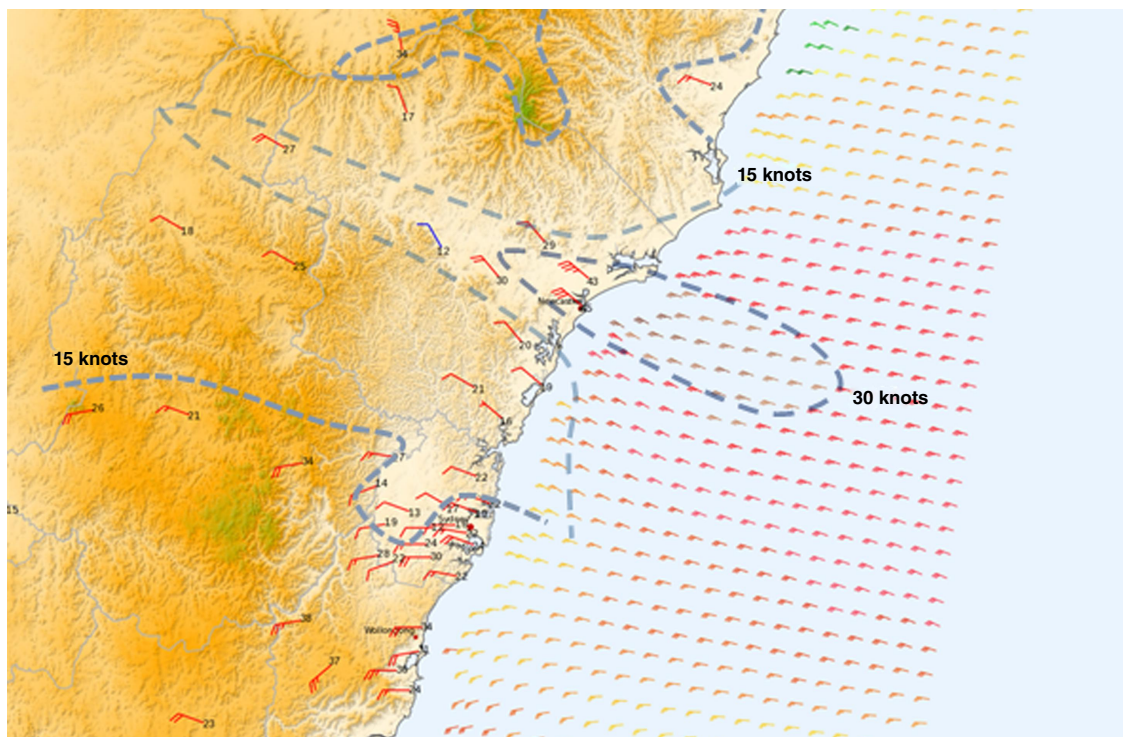


**Fig. 6.** The METAR map of the AWS and ASCAT winds over the Hunter Valley and the Hunter Coastal Water at 10:00 hours AEST (00Z) on 6 July 2016. A number next to each wind barb is the METAR gust speed. Isotachs are manually analysed every 15 knot ( $\sim 27.8 \text{ km h}^{-1}$ ) over the Hunter Valley and surrounding regions.

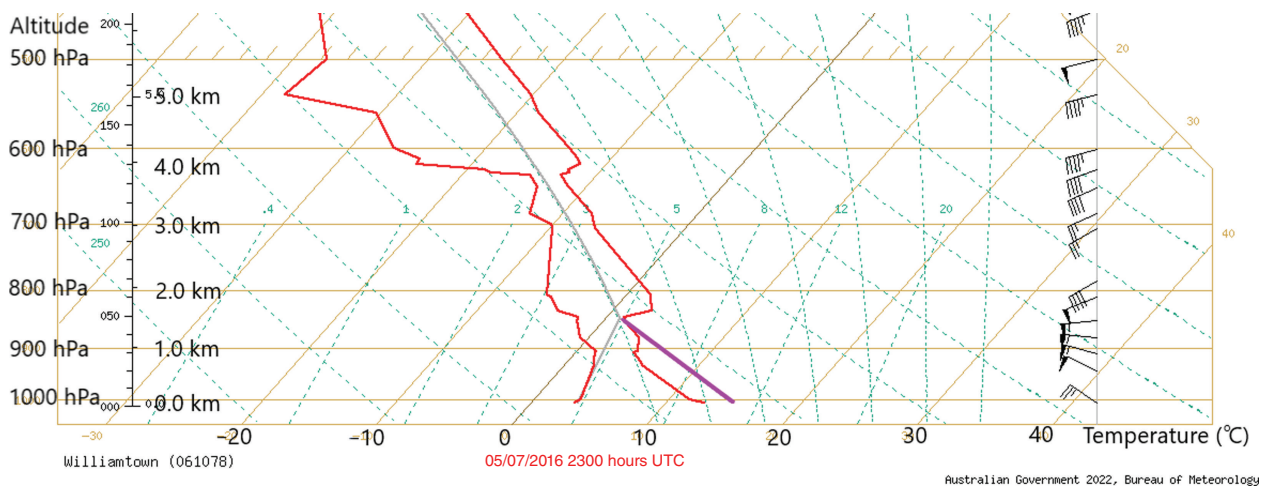


**Fig. 7.** Upper air sounding observation at Williamtown at 09:00 hours AEST (23Z) on 6 July 2016. The horizontal axis is the temperature ( $^{\circ}\text{C}$ ). Isotherms (solid diagonal lines) and dry adiabats (dashed diagonal lines) are marked for every  $10^{\circ}\text{C}$ . Upper-level winds are shown as wind barbs (knots) on the far right. Shown in purple is a construction of the boundary layer in the Lower Hunter at 12:00 hours, with a dry adiabat extending from the screen level temperature of  $15^{\circ}\text{C}$  at Williamtown.

Hunter stations and Merriwa gradually decreased through the late afternoon and evening (Fig. 5a, b), partly because of the cooling at the surface level and partly because of the backing of the geostrophic winds at the entrance of the valley. As the secondary low centre along the South Coast moved northward during the latter part of the day, the geostrophic winds further backed to SW as seen in the wind directions at Dubbo (Fig. 5c) and at the valley entrance where the decrease in  $u_0$  and the corresponding increase in  $v_0$  are observed after 18:00 hours (Fig. 5d). As it will be shown in Section 4.3, the increase in  $v_0$  leads to the deceleration of the channelled flow by Coriolis force. These changes explain the apparent decoupling of the wind speeds and  $\Delta p$  from 16:00 hours onwards.

## 4.2 Climatology of high-end wind events in the Hunter Valley

For this study, we define a *high-end wind event* as the event satisfying the following requirements: (1) at least one station in the Hunter Valley recorded the daily maximum wind gust greater than or equal to 44 knots ( $\sim 81 \text{ km h}^{-1}$ ), and (2) the same station or another station in the valley recorded METAR 10-min mean wind speeds greater than or equal to 22 knots ( $\sim 40 \text{ km h}^{-1}$ ) for 3 h or longer. The 44-knot ( $\sim 81.5 \text{ km h}^{-1}$ ) threshold was selected by allowing a 10% margin from the Bureau's wind-warning threshold. This 10% margin is in line with the required measurement uncertainty of wind gusts according to the World Meteorological Organization's (2021) 'Guide to Instruments and Methods of Observation'. Incidentally, 22 knots ( $\sim 40.7 \text{ km h}^{-1}$ ) is the Bureau's threshold for *windy* in the *précis* forecast. Excluding the observations at Murrurundi due to persistent strong winds by mountain-gap winds at the site, 69 wind events met both

(1) and (2) between July 2010 and June 2020. More than two-thirds occurred in winter (47 events, 68%), with the highest frequency in August (13 events) and the second highest in September (12 events). June was the third highest (9 events) and the month of the highest monthly frequency of ECL (Bureau of Meteorology and NSW Regional Office 2007; Callaghan 2021). Most of these events occurred in the Lower Hunter (64 events, 93%), with 11 events (16%) reporting 44 knots ( $\sim 81.5 \text{ km h}^{-1}$ ) or higher wind gusts in both Upper and Lower Hunters. Only 5 events (7%) occurred exclusively in the Upper Hunter. To investigate the relationship between the wind directions and the occurrence of the high-end wind events, wind roses of the surface-level winds and 850-hPa winds from the 69 events are constructed in Fig. 8. The surface-level wind direction of each event is represented by the direction of the highest wind gust in the valley since they were generally aligned with the prevailing mean wind directions in most events. The only exception was the 28 November 2018 event in which the direction of the second highest wind gust was used due to the highest wind gust being from thunderstorm outflow ahead of a southerly change. As for the 850-hPa wind rose, the vector average of 850-hPa reanalysis winds in both Hunters at either 00Z or 12Z was used – the nearer one to the timing of the occurrence of the highest wind gust. The surface wind rose (Fig. 8a) shows the primary peak along the WNW direction (26%), with 68% of wind directions within the WNW quadrant (WSW–NNW), pointing out the valley channelling as the main cause of the high-end wind events. The secondary peak in S–SSW directions is due to the maritime synoptic systems such as ECL, coastal trough or coastal southerly changes after frontal passage. The 850-hPa wind rose (Fig. 8b) exhibits a similar pattern, apart from the backing of the peak direction by  $1/16$  of a circle from the

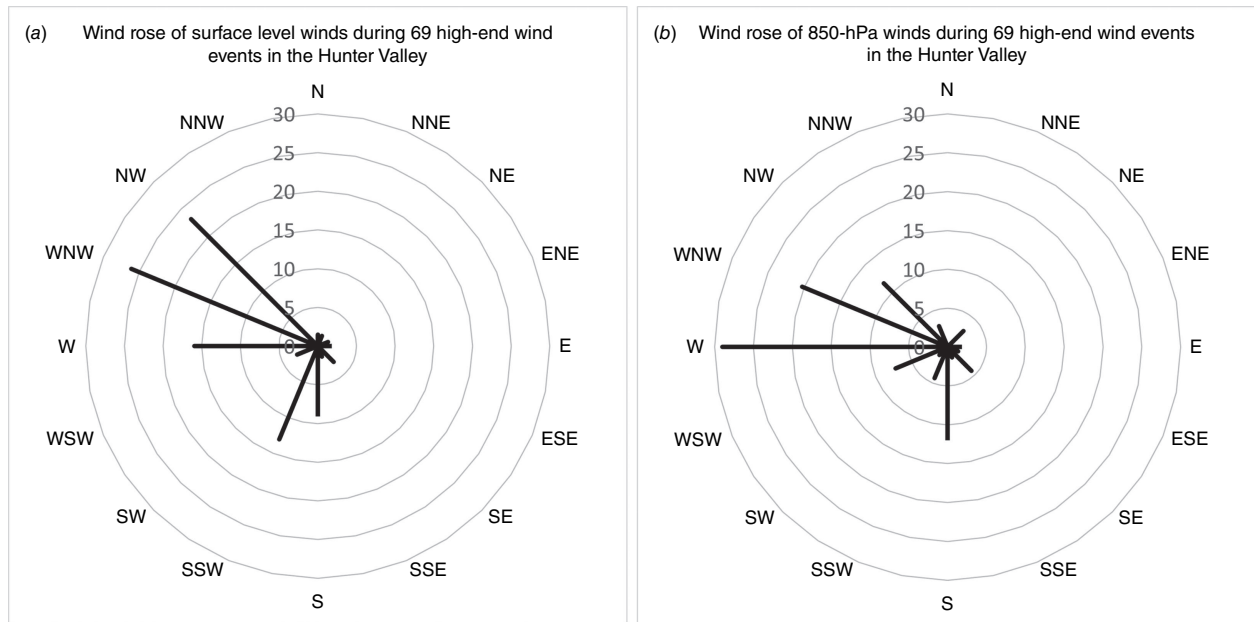


**Fig. 8.** Wind rose diagrams of the 10-m winds (a) and 850-hPa level winds (b) for the 69 high-end wind events between July 2010 and June 2020. Concentric rings are at a 5% interval.

peak direction at the surface level. The valley channelling and the frictional drag are thought to be the cause of this deviation between the peak wind directions at two levels. The peak at 850 hPa is found at W (29%), with the same 68% of wind directions lying within WSW–NW directions. In New South Wales, a frontal passage in winter brings westerly wind change, whereas north-west winds are generally pre-frontal both in winter and summer. The distribution of winds from the westerly quadrant at 850-hPa level suggests that high-end wind events are more likely in the post-front than pre-front. The fact that only a small portion of 850-hPa winds are from SW–WSW directions implies that the direction of the post-frontal airstream should not deviate too much from the valley axis to achieve high-end wind events. Although SW synoptic flow implies a larger pressure difference between the two ends of the valley, the overall effect appears to be a reduced likelihood of high-end winds because of the deceleration of the valley winds by Coriolis force that is proportional to the wind component normal to the valley axis. Further analysis on the causes of these 69 events and the types of valley channelling involved were carried out using the Bureau’s MSLP analysis chart archives, Global Position and Tracking Systems (GPATS) lightning strike map, SYNOPS and the upper air sounding data. The 47 westerly wind events were due to valley channelling, frontal passage or a combination of both. Among them, 26 events were due to pressure-driven channelling, 9 were due to other types of channelling such as downward momentum transport or forced channelling, and 12 were due to frontal passage or the combination of front and valley channelling. The 11 events that recorded gusts in both Upper and Lower

Hunters all involved frontal passage or thunderstorms in addition to valley channelling. The remaining 22 events were due to maritime synoptic systems that only affected coastal stations in the Lower Hunter. During the 10 years, the high-end wind events by maritime synoptic systems generally recorded stronger peak gusts (mean 49.8 knots,  $\sim 92.2 \text{ km h}^{-1}$ ) than valley channelling events (mean 48.5 knots,  $\sim 89.8 \text{ km h}^{-1}$ ). Destructive wind gusts (wind gusts exceeding 68 knots or  $\sim 125 \text{ km h}^{-1}$ ) were recorded only once in association with ECL on 21 April 2015 (Callaghan 2021). In summary, a high-end wind event in the Hunter Valley is most likely in the Lower Hunter during winter by pressure-driven channelling of westerly airstreams. Although wind events by maritime systems may bring more intense winds in the Lower Hunter, they are less frequent.

### 4.3 Strong westerly winds in the Lower Hunter by pressure-driven channelling

Fig. 9 shows the conceptual model of winter season pressure-driven channelling based on the synoptic or meso-scale features observed in the previous case study and the climatology of valley channelling in Sections 3 and 4.2. With SW–W airstreams in the wake of the frontal passage or when a low-pressure system develops over the south-western Tasman Sea, strong pressure gradient forms between the Upper and the Lower Hunter. A lee trough across the Upper Hunter through the Central Tablelands often forms in response to the SW–W airstream impinging on the Great Divide, and a weak ridge over the Northern Tablelands extends to the Upper to the mid-Hunter. These

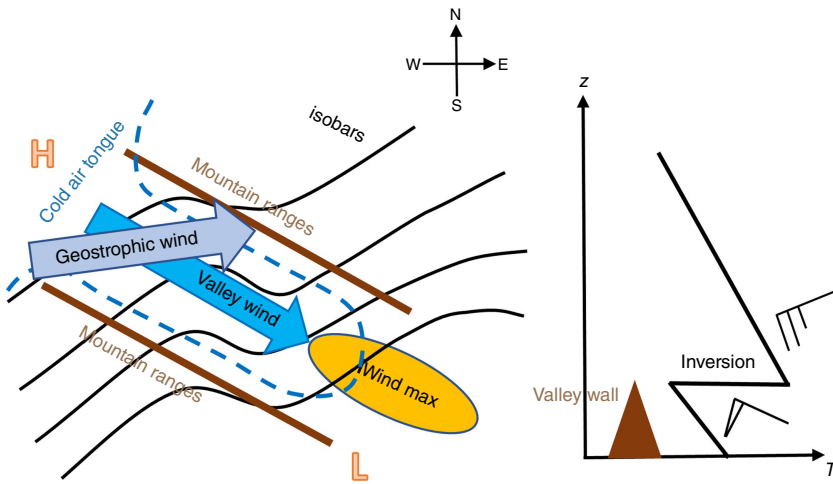


**Fig. 9.** Diagrams showing wind directions, isobars, the position of the wind-max, synoptic features, and aerological profile of wind and temperature for winter season channelling of westerlies in the Hunter Valley.

features appear to relax the pressure gradient along the valley. Under such synoptic conditions, upper air sounding at YWLM in winter often displays an inversion between 950 and 850 hPa due to the post-frontal nature of the channelled flow (Fig. 7 is an example). As the inversion height is comparable to the elevations of the valley walls (typically ~1000-m elevation), the flow is forced to follow the valley orientation while undergoing linear acceleration due to the pressure gradient force along the valley. A comparison of upper air soundings at Williamtown and Sydney airport suggests that the westerly winds channel a tongue of cold air through the valley (not shown), which lies underneath the inversion and possesses ~1–3°C cooler potential temperature than the ambient air. The density difference between the channelled flow and the ambient air suggests that the gravity force plays an important role. It modulates the acceleration of the cascading flow through the internal gravity wave, and such effect can be quantified in terms of the Froude number defined below:

$$r = \frac{\text{(speed of the low level jet)}}{\text{(phase speed of the gravity wave)}} = \frac{u}{\sqrt{g_r h}}$$

where  $g_r$  is the reduced gravity to the density difference between the cold air in the valley and the ambient air ( $\text{m s}^{-2}$ );  $h$  is the depth of the boundary layer (m).

As the flow is accelerated along the down-valley direction by both gravity and pressure gradient force, the flow speed comes to exceed the phase speed of the internal gravity wave at some point. Hence the flow experiences a transition from tranquil ( $r < 1$ ) to shooting ( $r > 1$ ). The wind-max should occur at the exit region around the Newcastle Metro and the surrounding coastal waters as the flow continues to accelerate before the flow eventually decelerates and merges with the ambient flow. With this, the flow becomes tranquil ( $r < 1$ ) again, and a type-2 hydraulic jump is thought to occur somewhere offshore, although it is hard to verify. This gravity-controlled wind process in the

Hunter Valley resembles katabatic winds observed in Antarctica, so its equations could be applied to construct a crude conceptual model. For example, in their earlier work, Grace and Holton (1988) looked at its application to Adelaide Gully Winds. Another justification is that the Hunter Valley is a wide valley with over 20 km wide. In general, valley walls exert a non-negligible influence on the flow (Wippermann 1984), especially when the valley is narrow. However, we adopt a simplified approach of a 2-D model with the assumption that the effect of the valley walls is only to force the winds to follow the orientation of the valley. With this, a heuristic relationship can be derived between the flow speed in the Lower Hunter, an indicative threshold of wind-warning conditions, and  $\Delta p$  under pressure-driven channelling.

Let  $x$  be the distance measured from the valley entrance along the valley axis,  $y$  be the distance from the valley axis along the cross-valley direction, and  $h$  be the depth of the well-mixed boundary layer flow (the down-valley motion of cold air ensures that the boundary layer is well mixed). Here,  $h$  should not exceed the heights of the valley walls by more than a few hundred metres. Otherwise, the assumption of the topographic constriction would not hold. The flow is also assumed to be steady, with the understanding that this assumption may fail with rapidly changing conditions like frontal passage. Let  $u$  and  $v$  be the flow speeds in the  $x$  and  $y$  directions respectively. The equations of motion (Ball 1956; Manins and Sawford 1979) are:

$$\begin{aligned} \frac{d}{dx}(hu) &= c_E u \\ \frac{d}{dx}\left(hu^2 + \frac{1}{2}g_r h^2\right) &= hF - c_D u^2 \\ F &= -\frac{1}{\rho} \frac{\partial}{\partial x} p + fv + g_r \alpha \end{aligned}$$

where  $F$  is the forcing term ( $\text{m s}^{-2}$ );  $c_E$  is the coefficient of entrainment;  $c_D$  is the coefficient of surface drag;  $\alpha$  is the

angle of inclination of the valley, positive for downward slope (rad);  $f$  is the Coriolis parameter ( $\text{s}^{-1}$ ).

For the actual calculation, the following values will be used for constants:  $\rho = 1.2 \text{ kg m}^{-3}$ ,  $c_D = 0.001$ ,  $c_E = 0.002$ . Further, in the context of the Hunter Valley, the following estimates will be used:  $L = 250 \text{ km}$ ,  $\bar{\alpha} = 0.002$ ,  $f = -7.8 \times 10^{-5} \text{ s}^{-1}$ ,  $\bar{h} = \sim 1000 \text{ m}$ . Also, our anecdotal experiences suggest  $g_r \sim 0.07 \text{ m s}^{-2}$  based on the potential temperature deficit of  $2^\circ\text{C}$ .

Solving for  $du/dx$  only, the equation simplifies as below:

$$\left(1 - \frac{1}{r^2}\right) \frac{d}{dx} \left(\frac{1}{2}u^2\right) = F - \frac{1}{h} \left(c_D + \left(1 + \frac{1}{r^2}\right)c_E\right)u^2$$

Denoting the average values of the parameters along the valley by overbars and the initial values of the wind speeds at the entrance by a subscript 0, the right-hand side of the equation simplifies to:

$$\left(1 - \frac{1}{r^2}\right) \frac{d}{dx} \left(\frac{1}{2}u^2\right) \cong \bar{F} - \frac{c}{\bar{h}}u^2$$

where:

$$\begin{aligned} \bar{F} &= -\frac{1}{\rho} \frac{\Delta p}{L} + \frac{1}{2}f v_0 + g_r \bar{\alpha} \\ c &= c_D + c_E \left(1 + \left(\frac{\bar{1}}{r^2}\right)\right) \cong c_D + \frac{3}{2}c_E \\ l &= \frac{\bar{h}}{c} \end{aligned}$$

and  $\Delta p$  is the pressure difference between the two ends of the valley;  $L$  is the length of the valley;  $\bar{\alpha}$  is the average inclination of the valley;  $(u_0, v_0)$  are the initial values of the along-valley ( $x$ ) and cross-valley ( $y$ ) wind components at the entrance;  $\bar{h}$  is the average boundary layer depth along the valley.

The quantity  $l$  defined above is the length scale of the frictional balance, which happens to be approximately the same order of magnitude as the length of the Hunter Valley. Trying  $r^2 \cong 1 + 8\sqrt{x} \div \bar{l}$  based on the empirical observation that  $r = \sim 1$  at the valley entrance and  $r = \sim 3$  at the valley exit in high-end wind events:

$$\begin{aligned} u(x) &\cong \sqrt{(1 - e^{-p(x)}) \frac{\bar{h}}{c} \bar{F} + u_0^2 e^{-p(x)}} \\ \left(p(x) &= \frac{2x}{\bar{l}} + \frac{1}{2} \sqrt{\frac{x}{\bar{l}}}\right) \end{aligned}$$

Denoting the values at the exit by a subscript f, the speed of the low-level jet at the exit is  $u_f = u(L)$ . The  $u(x)$  increases monotonically in  $x$ , with the rate of increase per unit distance faster in the Upper Hunter than the Lower Hunter. A comparison of  $u(x)$  value at Merriwa and Newcastle yields an 80% ratio, which overestimates the ratio by  $\sim 20\%$  in most cases. The faster increase in the Upper Hunter is due to

the assumption of an even pressure gradient along the valley. In reality, the pressure gradient is uneven. It is generally weaker in the Upper Hunter but stronger towards the Lower Hunter due to a weak ridging from Northern Tablelands. Nevertheless,  $u(x)$  is expected to converge to the actual flow speed in the Lower Hunter and nearby inshore coastal water while attaining the maximum speed there as it approaches asymptotically to the limiting speed  $\sqrt{\bar{h}\bar{F} \div c}$ . This solution also shows that  $u_f$  depends chiefly on  $\Delta p$  and  $(u_0, v_0)$ . It is broadly proportional to  $\sqrt{\Delta p}$ , provided that the direction of the upstream flow is between SW and WNW and that other factors are equal. The  $f v_0$  term in  $\bar{F}$  is negative and acts as a deceleration term due to the Coriolis force. Therefore, the direction of airstreams entering the valley should be preferably from W–WNW (i.e. small  $v_0$ ) for high-end wind events. This is consistent with the climatology in Section 4.2, which confirmed that there were only a few high-end wind events with 850-hPa wind directions from SW–WSW.

Among all components in  $\bar{F}$ , the pressure-gradient force is by far the largest. Hence the name pressure-driven channelling is appropriate. To see this point, suppose  $\Delta p = \sim 3 \text{ hPa}$  and that  $v_0 = \sim 5 \text{ m s}^{-1}$ , which typically brings  $\sim 30$ -knot ( $\sim 55.6 \text{ km h}^{-1}$ ) gust in the Lower Hunter. The magnitude and the relative percentage of each component of the forcing term in  $\bar{F}$  would be:

Terms	Interpretation	Magnitude ( $\times 10^{-4} \text{ m s}^{-2}$ )	Percentage
$-\frac{1}{\rho} \frac{\Delta p}{L}$	Pressure gradient force	10.0	75
$\frac{1}{2}f v_0$	Coriolis force	1.95	15
$g_r \bar{\alpha}$	Gravitational force	1.40	10

The percentage contribution of the pressure gradient force would be even more significant when  $\Delta p$  is greater than 3 hPa.

To verify the relationship between  $\Delta p$  and  $u_f$ , they are compared with the daily maximum wind gusts and the 12:00-hours SYNOP 10-min mean wind speeds from the pressure-driven channelling events between July 2010 and June 2020.

In selecting the events, the following criteria were applied since it was not feasible to scrutinise all 10-year observations individually:

- (1) The directions of the observed daily maximum wind gusts and the 12:00-hours SYNOP mean winds at all three stations in the Lower Hunter (NBB, YWLM, YMND) are between W and NW.
- (2) The wind directions of the upstream winds at 900-hPa level entering the valley are between SSW–WNW (i.e. between  $200$  and  $300^\circ$ ). It was discussed in Sections 3 and 4.2 that the geostrophic winds must be within this range for significant winds to happen by pressure-driven

channelling. The required range assumes the valley orientation along 115–295° with a 5° margin. The 00Z 900-hPa reanalysis wind directions at 32.00°S, 149.00°E (near Dunedoo) are used for this purpose.

- (3) Those events with  $\Delta p \leq 1$  hPa at 09:00 and 12:00 hours are excluded, as the  $\Delta p$  value is too low to be considered pressure-driven channelling in such instances.
- (4) The maximum wind gust must occur between 06:00 and 18:00 hours AEST. Although strong winds in the Hunter Valley may be possible during night-time, such occurrence is mainly due to convections (gusty showers or thunderstorms) or a rapidly moving cold front. Otherwise, the surface-level winds in the Hunter generally follow diurnal trends, with the wind speeds increasing rapidly a few hours after sunrise and reaching the peak between mid-morning and early afternoon as the low-level jet mixes down to the ground.
- (5) Only the observations from the winter season (April to September) are used to avoid strong westerly winds arising from heat-driven downward momentum transport.
- (6) To screen thermally forced winds, the event is excluded if the pressure difference arising from temperature contrast between the Upper and Lower Hunter at 03Z (13:00 hours AEST) is greater than the pre-existing pressure difference between the two ends of the valley at 09:00 hours AEST. The temperature contrast between the Upper and Lower Hunter promoted by widespread low cloud over the western side of the Great Divide and the clear sky over the Lower Hunter may induce its own pressure gradient, enhancing the overall pressure difference between the two ends of the valley. The pressure difference thus produced is given by (Whiteman and Doran 1993):

$$\Delta p_d = \frac{gHp_0}{R\bar{T}^2} \left[ \Delta T_0 + \frac{1}{2}(\gamma_2 - \gamma_1)H \right]$$

where  $H$  is the height of the valley walls;  $\bar{T}$  is the average temperature in the valley;  $p_0$  is the pressure at the ridgetop level;  $\Delta T_0$  is the temperature difference between the two ends of the valley at the ridgetop level;  $\gamma_1, \gamma_2$  are lapse rates at the two ends of the valley ( $\text{K m}^{-1}$ ). Taking the ridge top level to be 900 hPa,  $H = 1000$  m,  $\bar{T} = 280$  K, and  $\gamma_1 = 0.005 \text{ K m}^{-1}$ ,  $\gamma_2 = 0.010 \text{ K m}^{-1}$ , it becomes  $\Delta p_d = 0.4$  hPa ( $\Delta T_0 + 2.5$ ) in the context of Hunter Valley. For each event,  $\Delta p_d$  is calculated by taking the difference of 900-hPa reanalysis temperatures between 32.90°S, 151.75°E (near Newcastle) and 32.00°S, 149.00°E (near Dunedoo). Then those events with  $\Delta p \leq \Delta p_d$  are excluded from consideration.

There could be some pressure-driven channelling events left out by this screening process, such as those that occurred in the summer season (October–March). Between July 2010 and June 2020, 508 events were identified as having met criteria (1)–(4). Among them, 361 events occurred during the winter season (April–September), and

147 events occurred during the summer season, implying that criterion (5) could potentially reduce the total number of cases by up to 30%. However, it is thought that the number of genuine post-frontal pressure-driven channelling events in summer seasons is few, as many of the summer season channelling events experience transitions from pressure-driven channelling to heat-driven downward momentum transport during the course of the day. Lastly, among the 361 events satisfying (1)–(5), 49 events were found to be thermally forced according to (6), leaving only 312 cases that meet all the criteria.

Fig. 10a shows a scatter plot of the daily maximum wind gusts  $v$ .  $\Delta p$  at 12:00 hours AEST for the 312 events, and Fig. 10b depicts a similar plot of 12:00-hours SYNOP (02Z) 10-min mean wind speeds  $v$ .  $\Delta p$  at 12:00 hours AEST for the same events. Wind observations are from the three AWS sites around the Newcastle Metropolitan area (YWLM, NBB, YMND), where the wind-max forms. Shown together in Fig. 10a, b are the curves of  $u_f$  (or 0.6 times of) as a function of  $\Delta p$  with initial values  $u_0 = 5.0 \text{ m s}^{-1}$  and  $v_0 = 5.0 \text{ m s}^{-1}$ . The  $u_0, v_0$  values chosen are within  $0.5 \text{ m s}^{-1}$  of the mean and medians of the  $(u_0, v_0)$  components of the 900-hPa reanalysis winds at the entrance. Inserted in Fig. 10 are the linear regression lines of the wind observations at YWLM for comparison purposes. The plots of  $u_f$  (or 0.6 times  $u_f$ ) closely follow the linear regression lines of Williamtown observations within the interval  $3 \leq \Delta p \leq 7$  hPa while nicely representing the general trends of the observed winds at all three stations across a wide range of  $\Delta p$ . Although the spread of observations from the graphs of  $u_f$  is noticeable, it is expected due to the spread of the actual values of  $\bar{h}, r, u_0$  and  $v_0$ . Also, some observations with significant deviations from  $u_f$  may have been due to the rapidly changing synoptic systems, for example, a fast-moving front or a rapidly developing low, or other types of channellings that were not completely filtered out. Despite them, the general agreement between  $u_f$  and the wind speed observations from the 312 events confirms that, when SW–WNW airstreams are channelled through the Hunter Valley by pressure-driven channelling, the observed wind speeds at the exit of the valley are broadly proportional to the square root of  $\Delta p$ , in agreement with  $u_f$ . The observations in the Lower Hunter, as well as the graph of  $u_f$  in Fig. 10a, b, suggest that  $\Delta p \geq 7$  hPa may be used as a first-hand guess of a wind-warning condition if we allow  $\sim 10\%$  margin, provided that the airstream entering the valley is from WSW–WNW rather than SW, although other factors such as rapid development or movement of synoptic features, or the depth of the boundary layer, should all be considered in making a decision before issuing an actual warning.

## 5 Conclusion

The climatology of valley channelling in the Hunter shows seasonal, spatial and directional variations for the dominant type of channelling. The prevalence of downward momentum

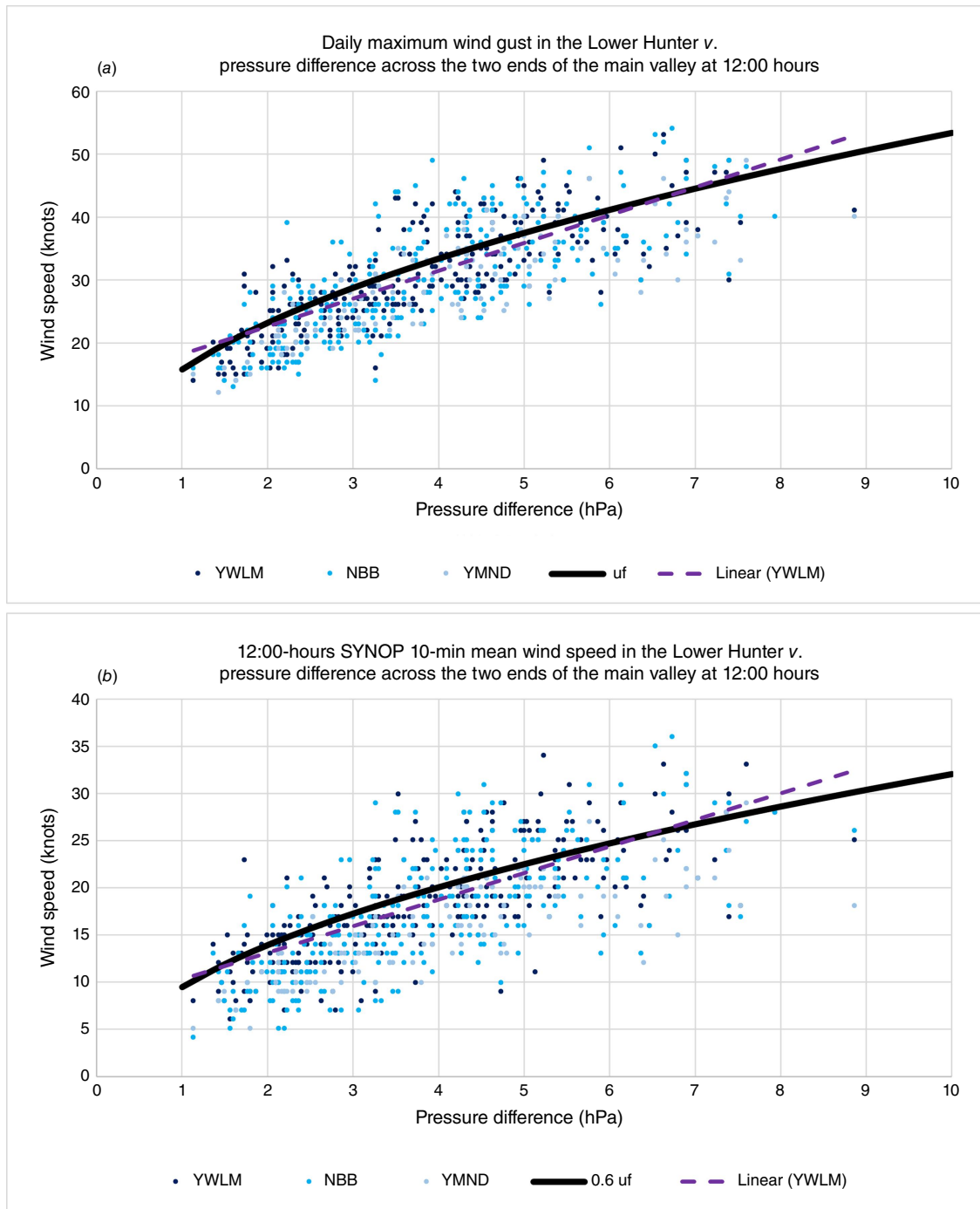


**Fig. 10.** Plots of surface-level winds in the Lower Hunter v.  $\Delta p$  at 12:00 hours AEST during the 312 pressure-driven channelling events in winter between July 2010 and June 2020. The winds used are (a) daily maximum wind gusts that occurred between 06:00 and 18:00 hours AEST (b) 12:00-hours SYNOP mean wind speeds. Dots are observations from Williamtown (dark blue), Nobbys Head (light blue) and Maitland (blue–grey). Also inserted in solid curves are the graphs of  $u_f$  (a) or  $0.6 u_f$  (b) with the initial values  $u_0 = v_0 = 5.0 \text{ m s}^{-1}$  and  $\bar{h} = 1000 \text{ m}$ . The purple dashed line is the line of the best fit based on the Williamtown observations.

transport in summer in the upwind region and the prominence of pressure-driven channelling in winter is due to the atmospheric stability or instability of the air mass involved. The SE channelling is more pronounced in the Upper

Hunter, with strong evidence of pressure-driven channelling, including counter current. NW valley channelling is more conspicuous in the Lower Hunter, especially in winter. The channelling types associated with W–NW valley winds

can be pressure-driven channelling, downward momentum transport, forced channelling or a mix of them. Further consideration of the synoptic features, the air masses involved and topography indicates that the primary channelling type associated with SSW–WNW airstreams in winter is pressure-driven channelling, whereas the dominant channelling type associated with SW–NNW airstreams in summer is downward momentum transport. Forced channelling also plays a role with airstreams from certain directions, such as SE–SSW airstreams in the Upper Hunter or WNW–NNW airstreams in the Upper and Lower Hunter. These findings indicate that pressure-driven channelling and downward momentum transport are the two main types of channelling in the Hunter Valley, which is consistent with the previous research on wide, flat-bottomed valleys with low sidewalls in other parts of the world, including the Upper Rhine Valley in Germany (Gross and Wippermann 1987), Tennessee Valley in USA (Whiteman and Doran 1993) and Saint Lawrence River Valley in Canada (Carrera *et al.* 2009).

Each channelling type poses a unique hazard with its associated synoptic feature and its combined effect with topography. Still, this paper only focused on the pressure-driven channelling of westerly airstreams in winter in view of wind-warning conditions. The climatology of high-end wind events in the Hunter Valley shows that it is the most important cause of damaging winds in the region, particularly in the Lower Hunter. The same climatology and consideration of the Coriolis Effect confirm that westerly airstreams are more likely to produce wind-warning conditions in the Lower Hunter than south-westerly airstreams. When it happens, a distinct wind-max area is observed in the narrow area around Newcastle and the nearby coastal waters at the eastern end of the valley, with the wind speeds in the area generally proportional to the square root of the pressure difference between the two ends of the valley.

This paper presented a sketchy conceptual model of funneling, and future research may look into its application to other E–W oriented valleys in the eastern states of Australia, including the Goulburn–Kangaroo Valley corridor in New South Wales and the Lockyer Valley in Queensland, where similar amplification of westerly winds by topography is observed. Although this paper showed that wind-warning conditions in the Hunter Valley are less likely with north-westerlies in summer than with westerlies in winter, and quite unlikely with easterly airstreams all year around, other types of hazards (e.g. fire danger or aviation hazards) associated with airstreams from these directions could be the topics of future research.

## Supplementary material

Supplementary material is available [online](#).

## References

- Australian Institute for Disaster Resilience (2017) 'Major Incidents of the year 2016–2017'. (AIDR)
- Ball FK (1956) The theory of strong katabatic winds. *Australian Journal of Physics* **9**, 373–386. doi:10.1071/PH560373
- Bureau of Meteorology NSW Regional Office (2007) About East Coast Lows. Available at <http://www.bom.gov.au/nsw/sevwx/facts/ecl.shtml>
- Callaghan J (2021) East coast lows and extratropical transition of tropical cyclones, structures producing severe events and their comparison with mature tropical cyclones. *Journal of Southern Hemisphere Earth Systems Science* **71**(3), 229–265. doi:10.1071/ES21003
- Carrera ML, Gyakum JR, Lin CA (2009) Observational study of wind channelling within the St Lawrence River Valley. *Journal of Applied Meteorology and Climatology* **48**, 2341–2361. doi:10.1175/2009JAMC2061.1
- Grace W, Holton I (1988) A mechanism for downslope winds with special reference to the Adelaide Gully winds. *Meteorological Note* **179**, Bureau of Meteorology.
- Gross G, Wippermann F (1987) Channeling and countercurrent in the Upper Rhine Valley: numerical simulations. *Journal of Applied Meteorology and Climatology*. **26**(10), 1293–1304. doi:10.1175/1520-0450(1987)026<1293:CACITU>2.0.CO;2
- Hersbach H, Bell B, Berrisford P, *et al.* (2020) The ERA5 global reanalysis. *Quarterly Journal of the Royal Meteorological Society* **146**, 1999–2049. doi:10.1002/qj.3803
- Manins PC, Sawford BL (1979) A model of katabatic winds. *Journal of Atmospheric Sciences* **36**, 619–630. doi:10.1175/1520-0469(1979)036<0619:AMOKW>2.0.CO;2
- Matthews C, Lawrence S, Jardine R, Webb C (2002) Fog forecasting at Sydney Airport. In '2002 Weather Services Scientific Conference: extended abstracts', 3 June–7 June 2002. pp. 58–59. (Bureau of Meteorology, Service Branch)
- Muñoz Sabater J (2019) ERA5 hourly data on pressure levels from 1981 to present. (Copernicus Climate Change Service, C3S, and Climate Data Store, CDS) Available at <https://www.ecmwf.int/en/forecasts/datasets/reanalysis-datasets/era5> [Verified 2 July 2020]
- Weber RO, Kaufmann P (1998) Relationship of synoptic winds and complex terrain flows during the MISTRAL field experiment. *Journal of Applied Meteorology*. **37**, 1486–1496. doi:10.1175/1520-0450(1998)037<1486:ROSWAC>2.0.CO;2
- Whiteman CD, Doran JC (1993) The relationship between overlying synoptic-scale flows and winds within a valley. *Journal of Applied Meteorology* **32**, 1669–1682. doi:10.1175/1520-0450(1993)032<1669:TRBOSS>2.0.CO;2
- Wippermann F (1984) Air flow over and in broad valleys: channeling and counter-current. *Beitraege zur Physik der Atmosphaere* **57**, 92–105.
- World Meteorological Organization (2021) Chapter 1. Annex1.A. Operational measurement uncertainty requirements and instrument performance requirements. In 'Guide to Instruments and Methods of Observation, Vol. 1. Measurement of Meteorological Variables'. pp. 25–34. (WMO) Available at [https://library.wmo.int/doc\\_num.php?explnum\\_id=11612](https://library.wmo.int/doc_num.php?explnum_id=11612)
- Zhong S, Li J, Whiteman CD, Bian X, Yao W (2008) Climatology of high wind events in the Owen Valley, California. *Monthly Weather Review* **136**, 3536–3552. doi:10.1175/2008MWR2348.1

**Data availability.** The surface observation data (METAR and SYNOP) and the upper air sounding data at Williamtown RAAF that support this study were obtained from the Bureau of Meteorology, Australia. They are either available either free of charge from the Bureau's website <http://www.bom.gov.au> or can be requested with charges at cost recovery basis at <http://www.bom.gov.au/climate/data-services/station-data.shtml>. The ERA5 reanalysis data that support this study were obtained from ECMWF, and they can be accessed at <https://cds.climate.copernicus.eu/cdsapp#!/dataset/reanalysis-era5-pressure-levels?tab=overview>.

**Conflicts of interest.** The authors declare that they have no conflicts of interest.

**Declaration of funding.** This research did not receive any specific funding.

**Author affiliations**

<sup>A</sup>Formerly at Williamtown Weather Services Office, Bureau of Meteorology.

<sup>B</sup>NSW and ACT Decision Support Service, Bureau of Meteorology, Sydney, NSW, Australia.